On the electrooxidation of glucose on gold: towards an electrochemical glucaric acid production as value-added chemical

Nicolas Schlegel, Gustav K. H. Wiberg, Matthias Arenz *

Department of Chemistry, Biochemistry and Pharmaceutical Sciences, University of Bern, Freiestrasse 3, 3012 Bern, Switzerland

* Corresponding author: matthias.arenz@unibe.ch

Abstract

The electrocatalytic oxidation of glucose to value-added chemicals, such as glucaric acid, has gathered increased interest in recent years. Glucose oxidation is a promising process which has the potential to contribute to establishing renewable resources as alternatives to fossil carbon sources. Herein, we present rotating disk electrode (RDE) studies on polycrystalline gold surfaces as a benchmark to expand the understanding of reaction kinetics and competition between glucose, reaction intermediates and OH^- at the catalyst surface. Combining electrochemical studies and Raman spectroscopy, it is shown that increasing glucose concentrations lead to a delayed oxidation of the gold catalyst surface, presumably by increased consumption rates of Au-hydroxide species.

Keywords

Glucose oxidation reaction; Gold electrode; glucaric acid; gluconic acid; value-added chemical production

1. Introduction

Gluconic and glucaric acids, both Glucose derivatives, have received increased attention after being labelled top value-added chemicals by the U.S Department of Energy[1]. Gluconic acid finds its main application in the food industry, while also being used in pharmaceutical and hygienic products[2]. Glucaric acid is a precursor of adipic acid, an immensely important commodity chemical, renowned for being a building block for Nylon[3]. In the future, these glucose derivatives could be introduced as an alternative carbon source in the chemical industry, thereby contributing to the development of a closed anthropogenic carbon-cycle and the independence from fossil resources.

Historically, synthesis methods for gluconic and glucaric acid require harsh conditions demanding high temperatures, strong oxidants (NaBr and NaOCl[4,5]) and struggle with product selectivity. Alternatively, an electrochemical conversion approach can promise milder reaction conditions for the oxidation and can potentially make use of peak surplus renewable electricity. Furthermore, when the oxidation is done electrochemically, the product distribution is a function of the applied overpotential. Other key parameters for the product selectivity include the nature of the catalytic electrode and ad-atoms there on as well as the availability of hydroxide ions[6–8]. The most promising catalyst materials to date have been found to be Gold[9–14] and Platinum[15–18], which readily oxidize glucose in alkaline medium.

The electrochemical glucose oxidation typically generates a host of products. For example, Kokoh et al.[15] detected small carboxylic species, formed by breaking C-C bonds in the glucose, showing that gluconic acid is not the final oxidation product. Moggia et al.[19] recently reported that gold is able, in a two-step oxidation, to convert glucose to glucaric acid, with the reaction intermediate being gluconic acid. This makes gold an even more desirable catalyst material.

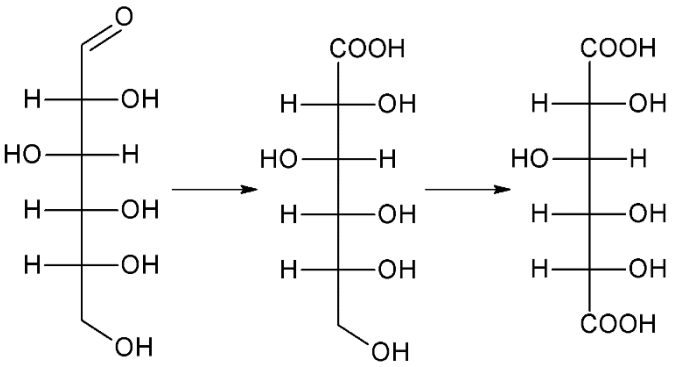

Figure 1: *Proposed two step oxidation from glucose to glucaric acid via gluconic acid.*

The general reaction mechanism of the glucose oxidation has been at the heart of a number of investigations[20–24]. A key step in the oxidation mechanism of glucose on gold catalysts is the formation of an OH-ad-atoms species and the availability of OH^- at the catalytic interface in general[25]. Hence, alkaline conditions have long been considered optimal. Rotating disk electrode (RDE) studies on polycrystalline gold electrodes by Larew and Johnson[12] found that the surface oxide formation caused

deactivation of the gold electrode. To complicate the matter, the deactivation also depended on the glucose concentration. More specifically, with increasing glucose concentration the gold oxidation was shifted to more positive overpotentials. The authors have ascribed this phenomenon to adsorbed glucose molecules blocking the gold surface.

The behaviour of glucose oxidation on metal electrodes has proven to be complex. Oscillatory behaviour has been observed[26–28], similar to other small organic molecules such as methanol[29], ethylene glycol[30] and formic acid[31]. These oscillations suggest temporary surface poisoning either by oxygenated species or glucose residue. Implications arise from this behaviour for the design of more efficient electrocatalysts as they should have a high tolerance for these poisoning species and be able to catalyse more than just one of the reaction steps if glucaric acid is the desired product.

Hence, more insight on these results is still required for the design of an efficient reactor as finding stable electrolysis conditions turns out to be challenging. Potential programs involving three steps have been discussed: First, at low potential, the glucose adsorbs on the catalyst surface. In a second step, the glucose is then oxidized and later, in the third step at very high potentials, the surface is cleaned from all adsorbed species. This stepped program is then repeated for the duration of the operation[32]. Future more elegant solutions are expected to be helpful to increase the catalyst's overall efficiency.

This present work seeks to expand and advance the understanding of the reaction kinetics of the glucose oxidation reaction on gold, especially in the potential region close to the deactivation through gold oxidation. RDE setup using cyclic voltammetry and galvanostatic electrolysis provide the bulk of the experimental data. An RDE approach was chosen as it became obvious that mass transport limitations are reached easily in the glucose oxidation reaction. Operation under mass transport limitations would have meant the loss of valuable insight that influences the design of prospective catalysts and electrolysis set-ups. With the gathered insight we deem to identify several key aspects for an efficient electrochemical conversion set-up.

2. Experimental

Chemicals & Reagents

Ultra-pure water (MiliQ-systems, 2.7 ppb TOC, 18.2 MΩ) was used for all cleaning purposes and to prepare the supporting electrolyte adding sodium hydroxide monohydrate (≥99.99 %, suprapur, Merck) and sodium sulfate (≥99.0 % Sigma Aldrich). D-glucose (≥99.5 %) and the D-gluconic acid sodium salt (≥99.0 %) were also obtained from Sigma Aldrich. Argon gas (≥99.99 %, PanGas) was used to purge the electrolyte before experiments and to create slight overpressure in the headspace during operation. The Argon was also used to dry electrode tips and cell parts. Sodium sulfate was added to the electrolyte to yield a final concentration of 0.1 M with the purpose of ensuring sufficient electrolyte conductivity, thereby minimising internal resistances in the electrochemical setup.

Electrochemical set-up

A polycrystalline gold-disc (0.196 cm^2) embedded in Teflon served as the working electrode for the RDE studies. The working electrode was polished in an alumina slurry (0.3 my MicroPolish, Buehler) on a polishing cloth (MicroCloth, Buehler) followed by sonicating two times in high-purity water for 3 min each. Then, the Teflon tips were mounted onto a EDI101 rotating disk electrode assembly (Hach-Lange), which was controlled by a CTV101 speed control unit (Radiometer analytical) that was connected to the potentiostat software via plug-in. Furthermore, gold mesh was used as counter electrode. Then the reference electrode, a trapped hydrogen electrode, was produced in-situ by applying -8.00 mA to a dedicated Pt-wire, which was situated in a glass tube.

All RDE experiments were performed in a custom-built one-compartment glass cell (Figure S1). For cleaning, the cell was boiled in 25% HNO_3 followed by boiling twice in ultra-pure water. Between individual experiments the cell was thoroughly rinsed and boiled with ultra-pure water. After filling the electrolyte into the cell, it was purged with Argon gas for 25 min. Potential and electrical current were controlled with an ECi-210 potentiostat using the software EC4 DAQ 4.2, (both Nordic Electrochemistry

ApS). Thereafter, the reactant was introduced to the cell, followed by 15 min continued purging with Argon gas.

In order to minimize the potential error due to the iR-drop, before starting the experiments, the solution resistance of the setup was determined by electrochemical impedance spectroscopy (EIS) and subsequently compensated for by following a standardised protocol. First, the working electrode potential was held at 0.3 V_{RHE}, in the double layer region of gold. An AC perturbation of 5 kHz and an amplitude of 10 mV was applied in order to measure the effective solution resistance online. An analogue feedback scheme of the potentiostat was applied, and the feedback increased until the control system was almost rendered unstable, as indicated by noise spikes in the frequency analysis of the measured signal. EIS was subsequently performed within a frequency range of 1kHz to 50 kHz and an amplitude of 10 mV. From this measurement the apparent solution resistance was determined to be less than 3 Ω.

Raman spectroscopy

The Raman spectroscopy experiments were conducted with a LabRAM HR800 confocal Raman microscope (Horiba Jobin Yvon) and a custom-built polychlorotrifluoroethylene Kel-F cell (Figure S2) used previously[33]. The excitation laser wavelength was 633 nm, typically operating with a power of 17 mW. A 10x magnification long-working-distance objective (10.5 mm) was used to focus the laser onto the sample and to collect the scattered light in a backscattering geometry. The collection time of the Raman spectra was typically 1 second. The WE, a polycrystalline gold bead electrode was aligned parallel to the quartz-window (EMATAG AG). A coiled Pt-wire was used as counter electrode, a leakless micro Ag/AgCl (ET069-1, eDAQ) reference electrode was used, and the potential was controlled using an ECi-100 potentiostat (Nordic Electrochemistry ApS). Working electrode and electrolyte were treated identically as

in the RDE experiments, the only alteration was that the Ar purging took place in an external bubbler from which the electrolyte then was pumped into the electrochemical cell.

3. Results and Discussion

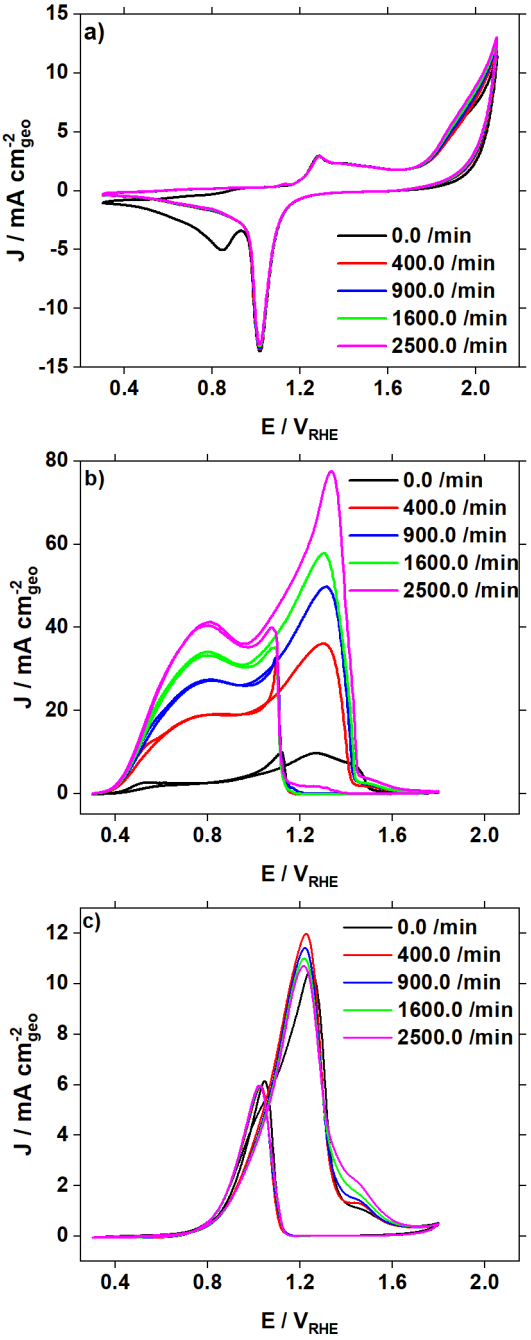

Figure 2: Cyclic voltammograms recorded with a scan rate of 50 mV s^{-1} on a polycrystalline Au-RDE in 0.1 M NaOH and 0.1 M Na_2SO_4; a) without glucose; b) 50 mM glucose; c) 50 mM gluconic acid. All measurements were recorded at room temperature.

We start the discussion of the results with the cyclic voltammograms (CV) of a polycrystalline gold disc-electrode in the base electrolyte, i.e., the 0.1 M NaOH + 0.1 M Na_2SO_4 aqueous electrolyte without glucose, see Figure 2a. The CVs serve as reference for the interaction of Au with the base electrolyte, knowledge that is important for the discussion of the reaction pathway of the glucose oxidation. In the positive going scan, between 0.3 and 1.2 V_{RHE} the typical double layer region of Au is observed followed by a distinct peak after ca. 1.25 V_{RHE}, which can be attributed to the formation of gold hydroxide-species[34]. At potentials > 1.8 V_{RHE} overlap of oxygen evolution (OER) and gold oxide (AuO_2) formation is observed. Reversing the scan direction, the oxidized Au-electrode reduces to metallic gold at ca. 1.1 V_{RHE} after which once more the double layer region is observed. The hysteresis between the formation and reduction of gold points towards an irreversible and rather sluggish process. In the absence of glucose (see Figure 2a) different rotation rates do not significantly influence the features of the voltammograms. Only slight deviations in current density are seen in the potential region of the OER. Furthermore, if the Au electrode is not rotated, the evolved oxygen in solution leads to a small oxygen reduction reaction current and concomitant “bending” of the CV after the Au reduction peak. This can be explained by the fact that when forced convection is applied the evolved oxygen is transported away from the interface and can therefore not be observed in the CVs.

When glucose is introduced to the cell, Figure 2b, two distinct new peaks are observed in the forward going scan. The maximum of the first peak is observed at 0.8 V_{RHE}, whereas the maximum of the second is peak observed between 1.3 and 1.35 V_{RHE}. The two peaks are followed by the deactivation of the Au surface towards the glucose oxidation reaction (GOR). During the negative going backward scan a rather “abrupt” re-activation towards GOR at 1.1 V_{RHE} is observed. After the reactivation the currents observed during forward and backward scan are identical. Comparing the CV recorded in the base electrolyte to the CV recorded in the presence of glucose it becomes apparent that the oxidation state of the Au surface drastically influences its activity towards the GOR. The observed surface deactivation in the presence of glucose coincides with the formation of surface oxides in the base electrolyte at 1.25 V_{RHE}. Similarly, the surface re-activation overlaps with the observed reductive current in the base

electrolyte at 1.1 V_{RHE}. Hence, the reduction of the surface leads to its re-activation and once again the GOR sets in.

Concentrating on the two peaks that indicate glucose oxidation, as shown in Figure 2b, the magnitude of the peak currents depends on the rotation rate, but no clear-cut current plateau regions are present. This indicates that the oxidation glucose process at this concentration range is at a mixed kinetic-mass transport limited. The dependence of the peak current on the rotation rate strongly suggests that in contrast to most published work, investigating the reaction with forced convection is preferable in order to distinguish between kinetic and mass-transport limited processes. In previous work, the potential of the peak at 0.8 V_{RHE} was linked to the oxidation of glucose to gluconic acid, whilst the potential of the second peak seems to be related to the gluconic acid oxidation, possibly yielding glucaric acid[19]. To re-assess this hypothesis, we recorded CVs in the presence of gluconic acid instead of glucose, Figure 2c. The results support the hypothesis in so far that only the peak at 1.3 V_{RHE} is observed. It can be noticed that the oxidation currents of gluconic acid do not depend on the rotation rate. Instead, they even seem to slightly decrease with increasing rotation rate. These observations lead us to the conclusion that the gluconic acid oxidation process is purely kinetically controlled under the investigated experimental conditions. Additionally, a comparison between the current densities of glucose oxidation in Figure 2b and gluconic acid oxidation in Figure 2c implies that if the GOR proceeds via the “gluconic acid pathway”, the second peak in the CV is indeed due a parallel or competitive oxidation process of glucose and gluconic acid, respectively, as well as potential additional reaction intermediates. That is, in this potential region most likely both processes compete for active sites on the catalyst surface.

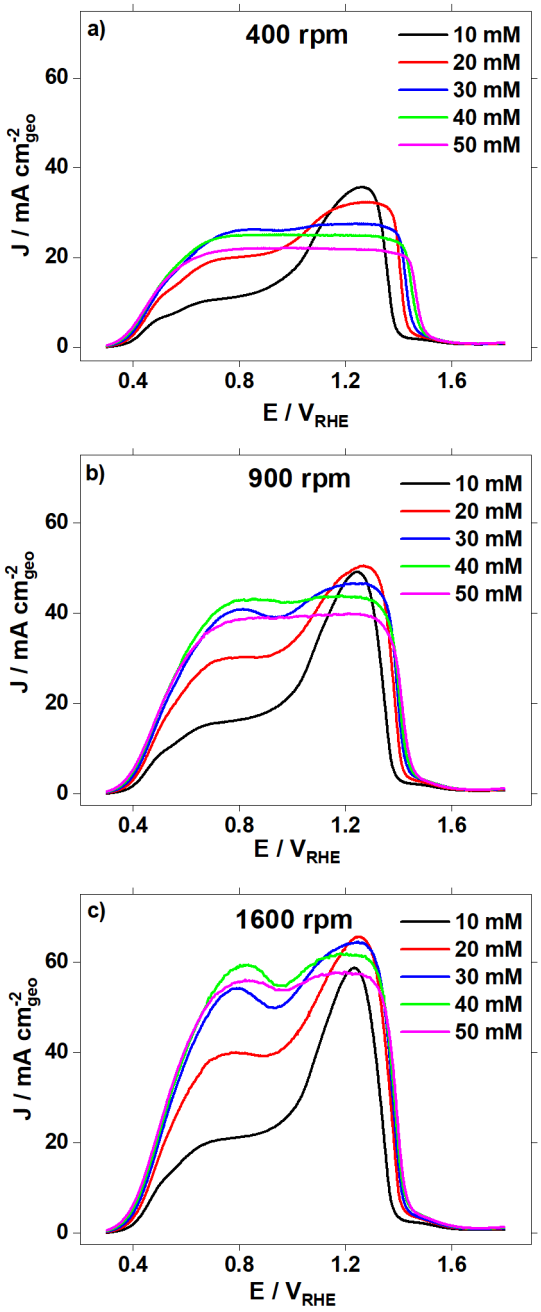

Figure 3: Cyclic voltammograms recorded with a scan rate of 50 mV s^{-1} on a polycrystalline Au-RDE (only forward scans are shown) in 0.02 M NaOH and 0.1 M Na_2SO_4 with 10mM - 50mM glucose added. a) 400 rpm; b) 900 rpm; c) 1600 rpm. All measurements were recorded at room temperature.

Next, we investigate the GOR in a lower hydroxide concentration. In Figure 3 CVs (only the forward scans are shown) recorded at different rotational rates with different glucose concentration in a 0.02 M NaOH (Figure S3 depicts rotation series for the individual glucose concentrations) and 0.1 M Na_2SO_4 base electrolyte are compared. In Figure 3a, where 400 rpm are applied, an oxidative current is observed, setting in after 0.4 V_{RHE}. For lower glucose concentrations (black and red line) a distinct second peak is observed after 1.2 V_{RHE}. For higher glucose concentrations (30 - 50 mM) a current

plateau is observed after reaching the respective maximum current at 0.7 V_{RHE}, which indicates that the predominant process is mass transport limited. At 30 mM glucose concentration (blue line) a small indentation can be seen at 0.9 V_{RHE}. Then, depending on the glucose concentration, a deactivation of the surface towards GOR occurs between 1.3 and 1.5 V_{RHE}. Interestingly, the maximum current density is inversely correlated to the reactant concentration as the highest and lowest maximum current density are recorded at 10 mM and 50 mM glucose, respectively.

Increasing the rotation rate to 900 rpm in Figure 3b increased current densities are measured, while the general shapes of the CVs closely resemble the CVs in Figure 3a. These observations match the ones from Figure 2. The indentation in the CVs recorded with 30 mM glucose concentration (blue line) has become more pronounced, also a small indentation can be observed at 40 mM glucose (green line). However, the maximum current density is notably different and is now observed at a glucose concentration of 20 mM (red line). At 1600 rpm (Figure 3c) no current plateaus are visible anymore, even the current density at 50 mM glucose concentration (magenta line) is slightly indent which means that no mass transport limitations are reached. The shapes of the CVs recorded with 10 to 30 mM glucose concentration do not change significantly as compared to Figure 2b and two distinct peaks attributed to the GOR are recorded.

We suggest that the observed CVs can be explained by a "three-way interaction" between OH^-, glucose and reaction intermediates (e.g. gluconic acid) at the surface. Because of the low hydroxide concentration of only 0.02 M in the electrolyte, OH^- at the solid-liquid interface is quickly depleted by the ongoing GOR. This hypothesis would explain the current plateaus observed for higher glucose concentration at lower rotational speed (Figure 3a) as the rate of mass transport to the surface is smaller than the rate of OH^- consumption thereat. Meanwhile, higher glucose availability at the interface, through higher starting concentrations, leads to higher rates of formation of reaction intermediates, presumably gluconic acid. The formed intermediates then compete with glucose for active sites on the gold surface. It was suggested that the peak at 1.2 V_{RHE} is an overlap of glucose and gluconic acid oxidation. However, our data show that these processes are controlled differently.

Glucose oxidation is mixed kinetic-mass transport limited whereas the oxidation of gluconic acid is shown to be kinetically controlled. The ratio between glucose and gluconic acid at the interface therefore influences the overall observed current. A comparison of the CVs recorded with 10 mM glucose concentration (black line) and with 50 mM glucose concentration (magenta line) from Figure 3a illustrates this point. The lower observed current density at 10 mM glucose concentration between 0.4 and 0.9 V_{RHE} indicates a lower rate of reaction intermediate (e.g. gluconic acid) formation than at 50 mM glucose concentration. Therefore, there is less competition for active sites at higher potentials which manifests itself in the higher current density at 10 mM glucose concentration. Shifting the mass transport limitations by increasing the rotation rate allows for higher maximum current densities at higher glucose concentrations (red CVs in Figure 3b, c).

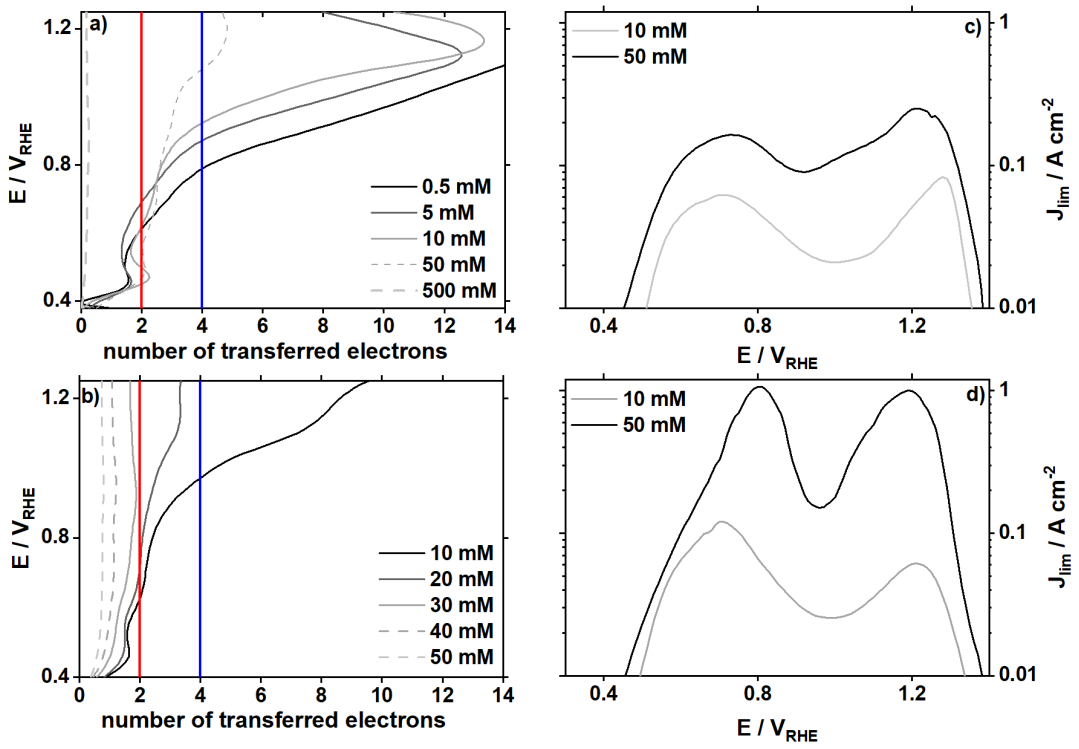

Figure 4: Koutecký-Levich analysis of RDE-measurement on an Au-disc in 0.1 M Na_2SO_4 and in different concentrations of glucose: a) numbers of transferred electrons in 0.1 M NaOH; b) kinetically limited current in 0.1 M NaOH; c) numbers of transferred electrons in 0.02 M NaOH; d) kinetically limited currents in 0.02 M NaOH.

Working with an RDE setup opens the possibility of deconvoluting kinetic and mass-transport processes. Using the Koutecký-Levich analysis[35] (Figure S4), we analyzed the data at every 5 mV from the recorded voltammograms by first plotting the data in a Koutecký-Levich plot at each specific potential as previously done by Zana et al.[36]. From the slope and y-axis-intersect we determined the so called Levich constant as well as the kinetically limiting current in the limit of infinite mass transport. Here we assume that the measured current is limited by the diffusion of glucose. From the Levich constant we calculated the numbers of transferred electrons using 6.7 x 10^{-6} cm^2/s as the diffusion coefficient for glucose and 0.01203 cm^2/s [12]as the electrolyte's viscosity. The results are shown in Figure 4.

For GOR the analysis shows that the number of transferred electrons depends on the applied voltage for both 0.1 M and 0.02 M NaOH concentration (Figure 4a and c). At glucose concentrations of 0.5 mM, 5 mM, 10 mM, and 50 mM in 0.1 M NaOH (Figure 4a), as well as 10 mM and 20 mM in 0.02 M NaOH (Figure 4c), the number of transferred electrons is close to two at potentials between 0.4 V_{RHE} and 0.6 V_{RHE}. Then an increase in transferred electrons is observed reaching its maximum at 1.2 V_{RHE}. At higher glucose concentration, specifically 500 mM in 0.1 M NaOH as well as 40 mM and 50 mM in 0.02 M NaOH the number of transferred electrons stays constant as a function of potential. Crucially, less than one electron is transferred per molecule of glucose.

To oxidize glucose to gluconic acid two electrons are required, to react gluconic to glucaric acid an additional four electrons must be transferred. Hence, to oxidize glucose to glucaric acid requires six electrons in total. It follows that glucaric acid is not the final oxidation product whenever more than six electrons are transferred. This can occur via the breaking of the carbon chain[15] and oxidising glucose fully to CO_2 requires 24 electrons[28]. As previously mentioned, the obtained data shows the number of transferred electrons changes as a function of potential (Figure 4 a and c), which indicates the occurrence of different oxidation processes at the gold surface: At small applied potentials, when only two electrons are transferred, gluconic acid is a likely product. When the applied overpotential is increased the number of transferred electrons drastically changes. In the case of 50 mM glucose concentration in 0.1 M NaOH (Figure 4a) approximately four electrons are transferred between 1.0 V_{RHE} and 1.2 V_{RHE}. Possible products include glucuronic acid, or glucaric acid from gluconic acid. At lower glucose concentrations (0.5 mM to 10 mM) in 0.1 M NaOH (Figure 4a) more than ten electrons are transferred. Possible products in these cases probably include small organic acids and CO_2. At 0.02 M NaOH a similar trend is observed: At 10 mM glucose concentration the transfer of more than ten electrons signifies the oxidation past glucaric acid. 20 mM and 30 mM glucose concentrations lead to the partial oxidation to a desired product. In case of higher glucose concentrations, the number of transferred electrons is smaller than one. These observations can be explained by OH^- scarcity at the catalyst surface which results in a fraction of glucose molecules arriving at the surface and leaving it

again unreacted. The same is the case for a glucose concentration of 500 mM in 0.1 M NaOH. The ratio of glucose concentration and hydroxide concentration is therefore an important measure for the glucose oxidation process as a delicate balance between OH^- and glucose concentration must be reached for the oxidation process to yield desired products: Sufficient OH^- has to be present at the surface for every reactant to react but OH^- must not be over-abundant for the reactant to become oxidized past glucaric acid.

In Figure 4b and d the apparent kinetically limited currents are shown for 10 mM and 50 mM concentration of glucose in 0.1 M NaOH and 0.02 M NaOH respectively. In both cases local maxima for the kinetically limited currents can be found. The first at approximately 0.7 V_{RHE} in the case of 0.1 M NaOH (Figure 4b) and at 0.8 V_{RHE} in the case of 0.02 M NaOH concentration. The second maximum is observed 1.2 V_{RHE}. In both cases, the obtainable current density correlates with the concentration of glucose: Higher glucose concentration leads to larger kinetically limited current densities. Interestingly, we calculated larger limiting current densities for 0.02 M NaOH concentration (1 A/cm^2) than at 0.1 M NaOH concentration (250 mA/cm^2). One would intuitively assume that higher OH^- availability would increase the achievable maximum current densities, however that does not seem to be the case.

Comparing the experimentally recorded current densities (Figure 2 and 3) to the maximum current densities calculated by means of the Koutecký-Levich analysis, the data indicate that under all experimental conditions the reaction is governed by mass transport limitations, even at high rotation speeds. This observation further supports the need for reaction application that make use of force convection. Also, if one wants to gather a deepened understanding of the underlying reaction mechanisms the effect of mass transport has to be considered and accounted for.

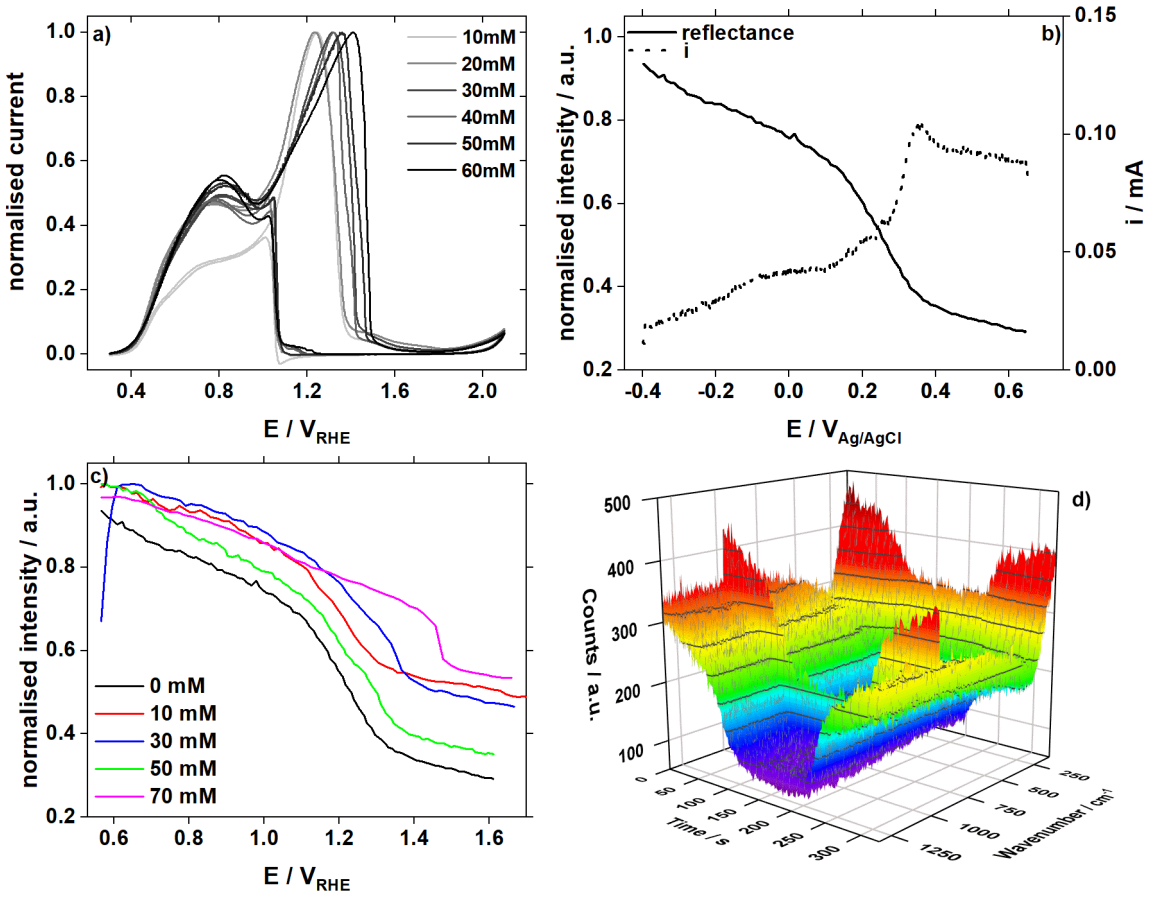

Figure 5: a) 10-60 mM glucose concentration in 0.1 M NaOH and 0.1 M Na_2SO_4 at 2500 rpm with normalized currents [J/J_{max}]; b) averaged recorded intensities (400 cm^{-1} to 890 cm^{-1}) as a function of potential (left y-axis) and corresponding CV recorded on Au-bead (right y-axis); c) comparison of averaged intensities at different glucose concentrations, 0 mM to 70 mM. d) colour map of Raman spectra continuously recorded during cyclic voltammetry (7 mV s^{-1}) in the absence of glucose. All measurements were recorded at room temperature.

The importance of OH^- availability at the catalyst surface is further illustrated by RDE-experiments on the Au-disc at glucose concentrations of 10 mM to 60 mM (Figure 5a). With increasing glucose concentration, the peak potential shifts from 1.23 V_{RHE} towards 1.5 V_{RHE}. Accordingly, the deactivation of the gold surface is also shifted towards larger overpotentials. Similar observations have been made by Larew and Johnson[12]. They suggested that this phenomenon is caused by surface blockage of adsorbed glucose. If this was the case, the current would not increase as a function of rotation but would be independent from it. However, as shown in Figure 2b, a clear dependence of the current on the rotation speed is observed. We suggest therefore, that the observed shift is caused by continuous consumption of adsorbed OH^-_{ads} which is a crucial species for the ongoing GOR. When increasing the glucose concentration, more reactant is transported to the catalyst surface leading to increased

consumption of already formed hydroxide species, thereby delaying the oxidation of gold. Upon further increase of the overpotential the driving force for the surface oxidation increases until the rate of oxide formation surpasses the rate of consumption. Finally, gold is oxidized and the surface becomes inactive. One concern with testing this hypothesis is the compensation of internal resistance in the electrochemical setup (iR drop). Insufficient or wrong compensation would lead to same observed shift in peak maximum. However, Figure 3a shows that the shift does not follow the current density but rather the glucose concentration. The highest maximum current density is recorded at a glucose concentration of 10 mM added to the base electrolyte, but the largest deactivation potential is observed at glucose concentration of 50 mM. Thus, the internal cell resistance can be ruled out as the primary cause for the shift in oxidation potential. The experiments performed at glucose concentrations of 20 to 40 mM confirm this trend: Higher glucose concentrations in the base electrolyte lead to larger deactivation potentials but smaller peak maxima.

Discussions of reaction mechanisms based on CVs are always limited. Therefore, Raman spectroscopy was used to follow the catalyst surface under reaction conditions and thus gaining spectroscopic insight about the surface state. In-situ measurements during cyclic voltammetry were conducted. Glucose at the interface proved to be difficult to detect due to its low normal Raman scattering (NRS) cross section[37], however, it was noticed that the oxidation state of the gold surface can be tracked, similar to what Pérez-Martinéz et al. have reported for glycerol oxidation on gold using visible reflectance and ATR-SEIRAS[38]. Raman spectra were continuously recorded in the range of 200 cm^{-1} to 1300 cm^{-1} while cycling a gold bead electrode between 0.57 and 1.67 V at 7 mV s^{-1}. At 981 cm^{-1} a characteristic sulphate peak (symmetric stretching)[39] stemming from the base electrolyte can be observed during the entire CVs, i.e., in the whole covered potential region. The surface reflectance, which we consider to be the background of the spectra, changes as the CVs progress. Figure 3a shows a colour map of the continuously recorded spectra during a CV. The reflectance dips into a well (blue part of the colour map) and returns to the initial intensity during the backwards scan. In the range of 400 cm^{-1} and 890 cm^{-1}, where no peaks are detected, the intensities were averaged to minimize the

influence of spike signals. Then the averaged intensity was plotted against the recorded CV, see Figure 3b, where an Au-bead electrode was cycled in the base electrolyte in the absence of glucose. In a first approximation the surface can be considered oxidized at the peak maximum at 1.35 V_{RHE}[34]. Accordingly, the averaged background reflectance has decreased. We therefore conclude that the observed change in reflectance is connected to the oxidation state of the gold surface: gold hydroxide exhibits a significantly lower reflectance than metallic gold. It follows that the reflectance can be used to observe the oxidation state of the gold electrode.

The experiment was repeated in the presence of different glucose concentrations (Figure 5c). The trend of delayed oxidation is observed through the reflectance in comparison to glucose free electrolyte (black line). A gradual shift towards higher oxidation potentials is visible from 10 mM (red), 30 mM (blue) to 70 mM (magenta) glucose. The spectra recorded in 50 mM (green) glucose do not match this trend (yet they are reproducible) with the reason being unclear to us. Nonetheless, the observed overall trend spectroscopically supports the electrochemical observation of delayed gold oxidation as a function of glucose concentration as the reactant temporarily hinders the formation of gold oxide

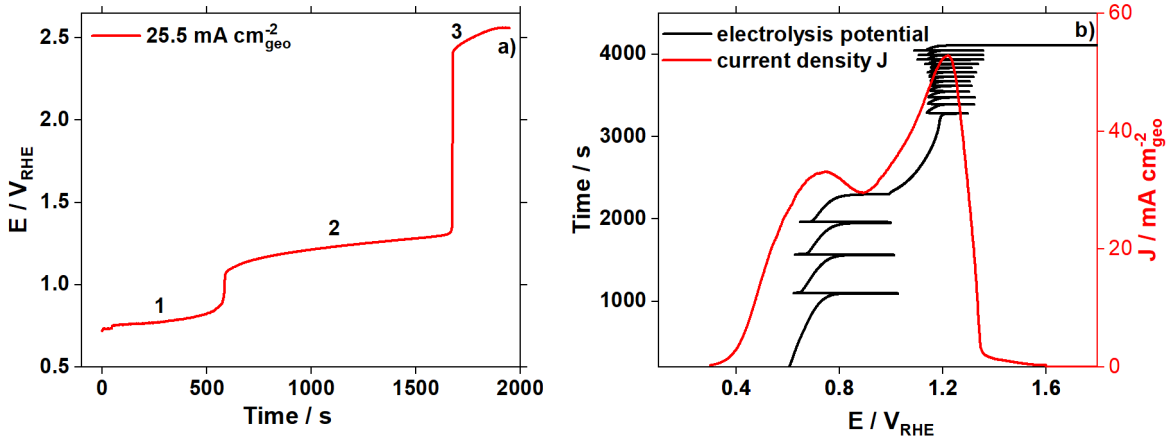

Figure 6: a) galvanostatic electrolysis measurement: 50 mM glucose, 0.1 M NaOH 25.5 mA cm^{-2} applied, rotating at 2500 rpm. b) galvanostatic electrolysis measurement: 50 mM glucose, 0.1 M NaOH 12.76 mA cm^{-2} applied, rotating at 2500 rpm. (left y-axis, black line). Steady-state CV recorded in 50 mM glucose at 2500 rpm (right y-axis, red line).

The complex nature of the glucose oxidation mechanism is showcased by Figure 6 and Figure 7. Galvanostatic electrolysis RDE-experiments on Au-discs were conducted where we observed three distinct potential regions at which the electrolysis takes place. This is depicted exemplary in Figure 4a. Three potential plateaus can be discerned labelled as (1)-(3): (1) 0.75 V_{RHE} – 0.88 V_{RHE}, (2) 1.1 V_{RHE} – 1.3 V_{RHE} and (3) >2.45 V_{RHE}. When the electrolysis takes place within the potential range of one of the observed plateaus, a very slow but steady increase in potential is observed. Upon reaching a potential threshold the electrolysis potential "jumps" abruptly to the next potential plateau with the progression in potential always going from the potential region (1) to (2) and finally plateau (3). The potential gradient ramping towards a threshold changes as a function of glucose concentration, applied current densities and rotation rates. Potential region 3 can be ruled out as a GOR-active potential because the gold surface is oxidized and therefore inactive towards glucose oxidation, as observed in Figures 1 and 2. Therefore it can be assumed that the recorded current is mainly due to the OER proceeding on the gold oxide surface. The potential ranges of (1) and (2) match the potentials of the peaks observed in the CVs as visualized in Figure 6b where the recorded electrolysis potential (black line) is plotted against a CV recorded with 2500 rpm (red line, right y-axis). It is clearly seen that the transition between potential plateaus coincides with the changes in the oxidation state of the gold surface. Thus, the electrolysis potential will never change back to a lower potential region because no "reducing potential" is applied to the catalyst surface. The introduction of rotation to the galvanostatic electrolysis increases the time before the catalyst becomes inactive towards the GOR and allows for significant current densities (25 mA cm^{-2}) to be applied, whereas without rotation the surface oxidizes almost immediately due to mass transport limitations. Based on these observations and the previously shown RDE experiments (Figure 2 and 3) electrolysis systems that enhance mass transport seem to be the most suitable candidates for the product-oriented oxidation of glucose.

Under galvanostatic conditions potential oscillations (Figures 6b, 7a, 7b) have been observed, in both potential regimes (1) and (2). The potential oscillations indicate temporary poisoning/blocking of the catalyst surface, followed by surface cleaning[26,28]. From Figure 6b it becomes clear that these

oscillations fluctuate around the peak potentials of the depicted CV, which coincide with glucose oxidation events as shown in Figure 1. Similar to Figure 6a, upon reaching a potential threshold, a transition to the next potential regime occurs.

We found the potential oscillations to be reproducible but not precisely controllable on the polycrystalline gold surface, indicating their structure sensitive nature. Frequency and amplitude are subject of change, also their manifestation in general. Figure 7 serves to illustrate this point: Figures 5a and 5b show individual experiments conducted under identical conditions. Yet, in Figure 7a the electrolysis takes place in the regime (1) for more than 1000 s, recording one major potential oscillation before transitioning to regime (2). In Figure 7b, regime (1) is "skipped entirely" reaching (2) after a mere 4 s. The potential gradually increases for 270 s before the potential starts to oscillate. For the next 500 s these oscillations continue, their amplitude being constant but their frequency increasing. After 800s of electrolysis, the system transfers to regime (3) when a sudden increase in potential leads to the oxidation of the surface, thereby becoming inactive towards the GOR. In contrast to the GOR, no oscillations have been observed when electrolyzing gluconic acid. It follows that the glucose itself is an important part of these oscillations. However, since two oscillatory regimes were identified, one can also conclude that there exists more than one feedback mechanism and that these mechanisms are either dependent on potential or that the feedback loop in (2) depends also on the surface oxidation state.

Last but not least, a potentiodynamic electrolysis approach for a technical, product-oriented GOR-process could be an interesting alternative to the often used three-step potential programs first introduced by Belgsir et al.[32]. Like the stepped potential programs, where the applied potential influences the product selectivity, the application of different current densities or rotation rates could be used to achieve similar effects. Allowing the potential to fluctuate during electrolysis could prove useful as the oscillations present a possible self-regenerating step for the catalyst surface, thereby increasing the catalyst's efficiency.

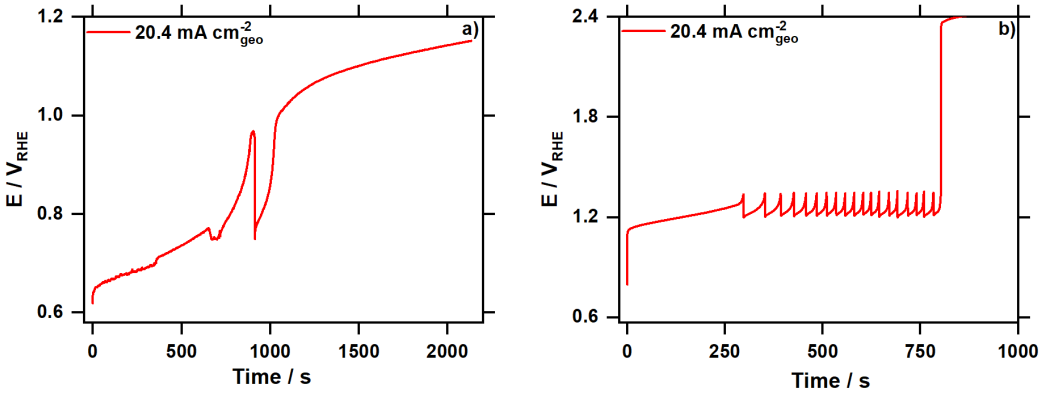

Fig. 7: a) and b): Two separate galvanostatic measurements at identical conditions: 50 mM glucose, 0.1 M NaOH, 20.4 mA cm^{-2} applied, 2500 rpm.

4. Conclusion

We can derive from our studies several key aspects for future glucose oxidation catalysts and electrolysis set-ups. From the combination of RDE studies supported by Koutecký-Levich analysis and spectroscopical investigations it becomes apparent that the oxidation of glucose is limited by mass transport, hence electrolysis set-ups with increased mass transport, such as flow-cells, need to be employed in future applications. Moreover, for gold surfaces we found the second oxidation step, correlating to the formation of gluconic acid, to be limiting the overall efficiency for converting glucose to glucaric acid. Consequently, if gluconic acid is a key intermediate, the catalyst design for glucose oxidation needs to focus on an efficient gluconic acid oxidation. To be efficient, catalysts need to shift the gluconic acid oxidation potential towards lower overpotentials. This can be achieved by incorporating different materials to the gold catalyst. Platinum is a reasonable candidate material in that regard as it is active towards gluconic acid oxidation several hundred millivolts earlier than gold[8,40]. Alloying[41–44] or preparing nanocomposites[45] of different metals, such as the already widely used gold and platinum, promises a combination of desirable material properties also in regards to product selectivity and distribution. The experimental evidence that the presence of glucose at the interface

shifts the gold oxidation towards higher potentials by competing for available OH^- with the gold surface might be key to improve the catalyst. The finding indicates that increased rates of glucose oxidation consuming adsorbed hydroxide species thereby delaying the formation of inactive gold oxides. Shifting the formation of OH species on the catalyst to lower potentials might help to create highly efficient catalysts for the GOR.

Acknowledgement

This work was supported by the Swiss National Science Foundation (SNSF) via the project No. 200021_184742.

References

1. Werpy, T. & Petersen, G. Top Value Added Chemicals from Biomass Volume I. *Us Nrel* (2004). doi:10.2172/15008859

2. Ramachandran, S., Fontanille, P., Pandey, A. & Larroche, C. Gluconic Acid: Properties, Applications and Microbial Production. *Food Technol. Biotechnol.* **44**, 185–195 (2000).

3. Van De Vyver, S. & Román-Leshkov, Y. Emerging catalytic processes for the production of adipic acid. *Catal. Sci. Technol.* **3**, 1465–1479 (2013).

4. Ibert, M., Marsais, F., Merbouh, N. & Brückner, C. Determination of the side-products formed during the nitroxide-mediated bleach oxidation of glucose to glucaric acid. *Carbohydr. Res.* **337**, 1059–1063 (2002).

5. Ibert, M. *et al.* Improved preparative electrochemical oxidation of d-glucose to d-glucaric acid. *Electrochim. Acta* **55**, 3589–3594 (2010).

6. Tonda-Mikiela, P. *et al.* Synthesis of Gold-Platinum Nanomaterials Using Bromide Anion Exchange-Synergistic Electroactivity toward CO and Glucose Oxidation. *J. Electrochem. Soc.* **159**, H828–H833 (2012).

7. Hebié, S., Napporn, T. W., Morais, C. & Kokoh, K. B. Size-Dependent Electrocatalytic Activity of Free Gold Nanoparticles for the Glucose Oxidation Reaction. *ChemPhysChem* **17**, 1454–1462 (2016).

8. Moggia, G., Kenis, T., Daems, N. & Breugelmans, T. Electrochemical Oxidation of d -Glucose in Alkaline Medium : Impact of Oxidation Potential and Chemical Side Reactions on the Selectivity to d -Gluconic and d -Glucaric Acid. *ChemElectroChem* **7**, 1–11 (2019).

9. Parpot, P., Muiuane, V. P., Defontaine, V. & Bettencourt, A. P. Electrocatalytic oxidation of readily available disaccharides in alkaline medium at gold electrode. *Electrochim. Acta* **55**, 3157–3163 (2010).

10. Escalona-Villalpando, R. A. *et al.* Electrodeposition of gold on oxidized and reduced graphite surfaces and its influence on glucose oxidation. *J. Electroanal. Chem.* **816**, 92–98 (2018).

11. Cho, S., Shin, H. & Kang, C. Catalytic glucose oxidation on a polycrystalline gold electrode with an amalgamation treatment (TM 05092). *Electrochim. Acta* **51**, 3781–3786 (2006).

12. A. Larew, L. & Johnson, D. C. Concentration dependence of the mechanism of glucose oxidation at gold electrodes in alkaline media. *J. Electroanal. Chem.* **262**, 167–182 (1989).

13. Biella, S., Prati, L. & Rossi, M. Selective oxidation of D-glucose on gold catalyst. *J. Catal.* **206**, 242–247 (2002).

14. Li, C. Y. *et al.* In Situ Monitoring of Electrooxidation Processes at Gold Single Crystal Surfaces Using Shell-Isolated Nanoparticle-Enhanced Raman Spectroscopy. *J. Am. Chem. Soc.* **137**, 7648–7651 (2015).

15. Kokoh, K. B., Leger, J. M., Beden, B., Huser, H. & Lamy, C. 'On line' chromatographic analysis of the products resulting from the electrocatalytic oxidation of D-glucose on pure and adatoms modified Pt and Au electrodes - Par II Alkaline medium. *Electrochim. Acta* **37**, 1909–1918 (1992).

16. Kokoh, K. B., Léger, J. M., Beden, B. & Lamy, C. 'On line' chromatographic analysis of the products resulting from the electrocatalytic oxidation of d-glucose on Pt, Au and adatoms modified Pt electrodes-Part I. Acid and neutral media. *Electrochim. Acta* **37**, 1333–1342 (1992).

17. Vassilyev, Y. B., Khazova, O. A. & Nikolaeva, N. N. Kinetics and mechanism of glucose electrooxidation on different electrode-catalysts. Part I. Adsorption and oxidation on platinum. *J. Electroanal. Chem.* **196**, 105–125 (1985).

18. de Mele, M. F. L., Videla, H. A. & Arvía, A. J. Potentiodynamic Study of Glucose Electro-Oxidation at Bright Platinum Electrodes. *J. Electrochem. Soc.* **129**, 2207–2213 (1982).

19. Moggia, G., Schalck, J., Daems, N. & Breugelmans, T. Two-steps synthesis of D-glucaric acid via D-gluconic acid by electrocatalytic oxidation of D-glucose on gold electrode: Influence of operational parameters. *Electrochim. Acta* **374**, 137852 (2021).

20. Vassilyev, Y. B., Khazova, O. A. & Nikolaeva, N. N. Kinetics and mechanism of glucose electrooxidation on different electrode-catalysts. Part II. Effect of the nature of the electrode and the electrooxidation mechanism. *J. Electroanal. Chem.* **196**, 127–144 (1985).

21. Dourado, A. H. B. *et al.* In situ FTIR insights into the electrooxidation mechanism of glucose as a function of the surface facets of Cu2O-based electrocatalytic sensors. *J. Catal.* **375**, 95–103 (2019).

22. Ishimoto, T., Hamatake, Y., Kazuno, H., Kishida, T. & Koyama, M. Theoretical study of support effect of Au catalyst for glucose oxidation of alkaline fuel cell anode. *Appl. Surf. Sci.* **324**, 76–81 (2015).

23. A.B. Mello, G., Cheuquepán, W. & Feliu, J. M. Investigation of reactivity of Pt basal planes towards glucose electro-oxidation in neutral solution (pH 7): structure-sensitivity dependence and mechanistic study. *J. Electroanal. Chem.* **878**, 114549 (2020).

24. Beden, B., Largeaud, F., Kokoh, K. B. & Lamy, C. Fourier transform infrared reflectance spectroscopic investigation of the electrocatalytic oxidation of D-glucose: Identification of reactive intermediates and reaction products. *Electrochim. Acta* **41**, 701–709 (1996).

25. Adzic, R. R., Hsiao, M. W. & Yeager, E. B. Electrochemical oxidation of glucose on single crystal gold surfaces. *J. Electroanal. Chem.* **260**, 475–485 (1989).

26. Ferreira, G. C. A., Napporn, T. W., Kokoh, K. B. & Varela, H. Complex Oscillatory Kinetics in the Electro-Oxidation of Glucose on Gold. *J. Electrochem. Soc.* **164**, H603–H607 (2017).

27. Delmonde, M. V. F. *et al.* Electrocatalytic efficiency of the oxidation of small organic molecules under oscillatory regime. *J. Phys. Chem. C* **120**, 22365–22374 (2016).

28. Gabriel B. Melle, Altair, T., Rafael L. Romano & Varela, H. Electrocatalytic Efficiency of the Oxidation of Ethylene glycol, Glycerol, and Glucose under Oscillatory Regime. *ChemRxiv. Prepr.* **1**, 1–18 (2020).

29. Nagao, R., Cantane, D. A., Lima, F. H. B. & Varela, H. The dual pathway in action: Decoupling parallel routes for CO 2 production during the oscillatory electro-oxidation of methanol. *Phys. Chem. Chem. Phys.* **14**, 8294–8298 (2012).

30. Sitta, E., Nascimento, M. A. & Varela, H. Complex kinetics, high frequency oscillations and temperature compensation in the electro-oxidation of ethylene glycol on platinum. *Phys. Chem. Chem. Phys.* **12**, 15195–15206 (2010).

31. Perini, N., Batista, B. C., Angelo, A. C. D., Epstein, I. R. & Varela, H. Long-lasting oscillations in the electro-oxidation of formic acid on PtSn intermetallic surfaces. *ChemPhysChem* **15**, 1753–1760 (2014).

32. Belgsir, E. M. *et al.* Electrosynthesis in aqueous medium: a kinetic study of the electrocatalytic oxidation of oxygenated organic molecules. *Electrochim. Acta* **36**, 1157–1164 (1991).

33. Fu, Y., Rudnev, A. V., Wiberg, G. K. H. & Arenz, M. Single Graphene Layer on Pt(111) Creates

Confined Electrochemical Environment via Selective Ion Transport. *Angew. Chemie - Int. Ed.* **56**, (2017).

34. Burke, L. D. & Nugent, P. F. The electrochemistry of gold: I. The redox behaviour of the metal in aqueous media. *Gold Bull.* **30**, 43–53 (1997).

35. Bard, A. J. & Faulker, L. R. *ELECTROCHEMICAL METHODS: Fundamentals and Applications*. *John Wiley & Sons, Inc.* **2**, 337-341 (2001).

36. Zana, A. *et al.* Accessing the Inaccessible: Analyzing the Oxygen Reduction Reaction in the Diffusion Limit. *ACS Appl. Mater. Interfaces* **9**, 38176–38180 (2017).

37. Yonzon, C. R., Haynes, C. L., Zhang, X., Walsh, J. T. & Van Duyne, R. P. A Glucose Biosensor Based on Surface-Enhanced Raman Scattering: Improved Partition Layer, Temporal Stability, Reversibility, and Resistance to Serum Protein Interference. *Anal. Chem.* **76**, 78–85 (2004).

38. Pérez-Martínez, L., Balke, L. & Cuesta, A. Reactive and inhibiting species in the electrocatalytic oxidation of glycerol on gold. A study combining in-situ visible reflectance and ATR-SEIRAS. *J. Catal.* **394**, 1–7 (2021).

39. Fontana, M. D., Mabrouk, K. Ben & Kauffmann, T. H. Raman spectroscopic sensors for inorganic salts. *Spectrosc. Prop. Inorg. Organomet. Compd.* **44**, 40–67 (2013).

40. Kokoh, K. B. *et al.* Selective oxidation of D-gluconic acid on platinum and lead adatoms modified platinum electrodes in alkaline medium. *Electrochim. Acta* **38**, 1359–1365 (1993).

41. Tominaga, M. *et al.* Electrocatalytic oxidation of glucose at gold-silver alloy, silver and gold nanoparticles in an alkaline solution. *J. Electroanal. Chem.* **590**, 37–46 (2006).

42. Habrioux, A. *et al.* Activity of platinum-gold alloys for glucose electrooxidation in biofuel cells. *J. Phys. Chem. B* **111**, 10329–10333 (2007).

43. Zhao, J., Wang, F., Yu, J. & Hu, S. Electro-oxidation of glucose at self-assembled monolayers

incorporated by copper particles. *Talanta* **70**, 449–454 (2006).

44. Jin, C. & Chen, Z. Electrocatalytic oxidation of glucose on gold-platinum nanocomposite electrodes and platinum-modified gold electrodes. *Synth. Met.* **157**, 592–596 (2007).

45. Du, J. *et al.* Bifunctional Pt-IrO2Catalysts for the Oxygen Evolution and Oxygen Reduction Reactions: Alloy Nanoparticles versus Nanocomposite Catalysts. *ACS Catal.* **11**, 820–828 (2021).